Physical-chemical and Biological Properties of Novel Resin-based Composites for Dental Applications

Zuzanna Buchwald (zuzanna.buchwald@put.poznan.pl)
Poznan University of Technology: Politechnika Poznanska https://orcid.org/0000-0001-8909-7926
Mariusz Sandomierski
Poznan University of Technology: Politechnika Poznanska
Wojciech Smułek
Poznan University of Technology: Politechnika Poznanska
Maria Ratajczak
Poznan University of Technology: Politechnika Poznanska
Adam Patalas
Poznan University of Technology: Politechnika Poznanska
Ewa Kaczorek
Poznan University of Technology: Politechnika Poznanska
Adam Voelkel
Poznan University of Technology: Politechnika Poznanska

Research Article

Keywords: hydroxyapatite, silica, resin-based composites, fillers

Posted Date: January 3rd, 2022

DOI: https://doi.org/10.21203/rs.3.rs-1200166/v1

Abstract

Insufficient mechanical properties of hydroxyapatite -based composites prompted the search for new and effective solutions for dental applications. To improve the mechanical properties without losing the remineralization potential, the use of hybrid fillers was proposed. The first of them was based on the formation of hydroxyapatite (HA) layer on the surface of SYLOID®244 silica. The second of the investigated fillers was created by simultaneous synthesis of nanoparticles from precursors of HA and silica. The obtained fillers were extensively characterized by spectral methods including X-ray Diffractometry (XRD), Fourier-Transform Infrared Spectroscopy (FT-IR), and X-ray fluorescence (XRF), as well as by Scanning Electron Microscopy (SEM)/Energy Dispersive Spectroscopy (EDS). Tests using probiotic microorganisms were an important part of the analysis, indicating that there was no potential interaction of the materials with microflora. The tests of degree of conversion, depth of cure, opacity, sorption, solubility, flexural and compressive strength, and the remineralizing potential also showed that the composites with nano-sized silica/HA showed better mechanical properties than the composites with HA alone or commercial silica and at the same time the remineralization remained at the desired level. Thus, the proposed composite has a high application potential in the creation of implants and dental materials.

Introduction

Calcium phosphates (CPs) are highly biocompatible [1-4], osteoconductive [2-4], and non-toxic [2] ceramic materials. Due to their excellent biological properties, calcium phosphates arouse wide interest from the point of view of medical applications, mainly as components of systems for bone regeneration [1]. In dentistry, they found application as components of products inducing remineralization, i.e. toothpaste, mouth rinses, chewing gums, etc. [3]. According to their remineralizing potential, understood as the ability to release calcium and phosphate ions, it is not surprising that attempts are made to apply calcium phosphates as bioactive fillers in resin-based composites to obtain restorative materials able to remineralize the surrounding tissues. Additionally, they are also cheaper than other currently used fillers [3]. The most widely examined CP filler is amorphous calcium phosphate (ACP) [5]. It is somehow surprising as ACP is highly soluble in water, which is both an advantage and disadvantage of this calcium phosphate. On the one hand, this high water solubility provides a high amount of ion released. However, on the other hand, it results in a weak mechanical strength of an ACP-filled composite. Moreover, the high ion release capacity is only apparently advantageous, as it lasts shortly (2-3 months) [5]. The most obvious choice, but not so well examined as ACP, is hydroxyapatite (HA). This choice is obvious due to the chemical similarity of synthetic HA to natural HA that builds teeth and bones [6-9]. Our previous research proved that HA can release calcium ions when incorporated into the organic matrix of methacrylic resin-based composites (RBC) [10]. Ca^{2+} release from HA-filled composites is long-term, as it lasts for at least 16 weeks [10]. Despite doubts on the potential mismatch of refractive indices between HA and methacrylic resins, the degree of conversion (DC), as well as depth of cure (DOC) of HA-filled composites are high [11]. In general, the main concern of CP-filled composites is related to the weak

mechanical properties [5,12]. Our previous research on mechanical properties of HA- and tricalcium phosphate (TCP)-filled RBC showed that both flexural and compressive strength should be improved [13]. The flexural strength of these composites was far from ISO 4049:2019 requirements, i.e. lower than 80 or even 50 MPa [14]. Also, compressive strength was below the values established as typical for RBC i.e. below 200-300 MPa, and far from the compressive strength of enamel (384 MPa) and dentin (295 MPa) [6].

In the current research, to overcome this issue, we propose to obtain hybrid fillers that combine HA and silica. Different types of inert silica are the most widely used fillers in dental composites [15-16]. Among others, silica is responsible for the excellent mechanical properties of such inactive composites. Our most recent study showed that the application of SYLOID®244 that consists of silica particles with high internal porosity and surface area, and narrow particle size distribution, results in the obtaining of RBC with extremely high compressive strength [17].

Therefore, combining bioactive HA showing the remineralizing potential with mechanically strong silica is highly justified. However, in the current research, the preparation of hybrid HA-silica fillers does not rely on the physical mixing them together, which could result in the lack of homogeneity. These hybrid fillers will be obtained in two different ways. The first consists of the preparation of the HA layer on the SYLOID®244 surface, obtaining, therefore, mechanically strong silica particles with an active HA surface layer. This method was used with success by our team to prepare zeolite and montmorillonite fillers with HA layer in the previous research [18-20]. All the obtained materials proved their remineralizing potential understood as the ability to release calcium ions with some weakness laying in their mechanical properties [18-20]. However, the prediction is that the silica particles will ensure the mechanical properties improvement of such type of fillers. This hypothesis is to be tested within the current research.

The second way of the preparation of a hybrid HA-silica filler that will be applied within this research is co-synthesis of silica and HA in a one-step method that was previously described by Hao et. al. [21]. It is predicted that in that way a homogeneous mixture of mechanically strong silica and bioactive HA nanoparticles will be obtained.

The aim of this study is to obtain hybrid HA-silica fillers by using two different methods, characterize and compare their basic properties, apply them as fillers in RBC, and examine the physicochemical properties of the obtained composites. The hypothesis of the research is that the hybrid fillers will ensure the improvement of the mechanical properties of the composites in comparison with HA-filled RBC with maintaining the remineralization potential of HA. To test this hypothesis, also the reference composite with only HA filler with the constant volume fraction will be prepared and examined as a reference. The properties of the composites according to the preparation methods of hybrid HA-silica fillers also will be compared.

Materials And Methods

Sodium hydroxide (NaOH), tetraethyl orthosilicate (98%; TEOS), sodium phosphate dibasic (99%, Na_2HPO_4), tris(hydroxymethyl)aminomethane (99.8%; Tris), hydroxyapatite (HA), bisphenol A glycerolate dimethacrylate (Bis-GMA), triethylene glycol dimethacrylate (95%; TEGDMA), camphorquinone (97%; CQ), ethyl 4-(dimethylamino)benzoate (≥99%; EDMAB), potassium hydroxide (≥ 85%, KOH), acetic acid (≥ 99.7%, CH_3COOH) were supplied by Sigma-Aldrich (Germany). Hydrochloric acid (36–38%, HCl) was obtained from Avantor (Poland). Calcium chloride of high purity ($CaCl_2$) and potassium phosphate monobasic (min. 99%, KH_2PO_4) were obtained from Chempur (Poland). SYLOID®244 was supplied by GRACE (USA).

Fillers preparation

Synthesis of silica-hydroxyapatite nanoparticles (n-SiO2-HA)

The synthesis was carried out according to Hao et. al. [21]. The scheme of the synthesis is presented in the Figure 1. In the first stage, 31.5 mL of a 0.2 M NaOH aqueous solution was added into 432 mL of water under stirring. Next, 0.574 g of Na_2HPO_4 was added to the solution. After 30 min of stirring at 70 °C, 4.05 mL of TEOS was added dropwise under vigorous stirring. Afterwards, 9 mL of solution containing 0.672 g of $CaCl_2$ was added. The reaction was kept at 70 °C for 4 h. The product was filtered and washed with H_2O. The last stage was calcination at 400 °C.

Preparation of silica (SYLOID®244) with hydroxyapatite layer (SYL-HA)

The methodology of hydroxyapatite mineralization was similar to that presented in our previous works [18-20]. SYLOID®244 (5 g) was immersed into 100 mL of 200 mM $CaCl_2$/Tris–HCl solution (pH 7.4) for 0.5 h. Then, the powder was filtered and washed with distilled water. In the second step, the material was placed into 100 mL of 120 mM Na_2HPO_4 solution for the same period of time (0.5 h). This process, consisting of two steps, was repeated five times. The last stage was calcination at 400 °C.

Fillers characterization

X-ray Diffractometry (XRD)

Prepared fillers were examined by the X-ray diffraction method in the range of 2 θ from 10 to 70 using a Bruker D8 Advance diffractometer with Johanson monochromator and LynxEye detector. Samples were measured in polymethyl methacrylate cuvette λ Cu Kα1=1,5406 Å.

Fourier-Transform Infrared Spectroscopy (FT-IR)

FT-IR analysis of all materials was carried out using Vertex70 spectrometer, Bruker Optics. Fillers were studied by using a single reflection, diamond ATR crystal. The tests were performed in the spectral range of 4000 – 600 cm^{-1} with a resolution of 4 cm^{-1} and 32 scans for signal accumulation.

Scanning Electron Microscopy (SEM) / Energy Dispersive Spectroscopy (EDS)

SEM images were recorded using TESCAN VEGA 3 SEM. SEM toll was equipped with an EDS XFlash detector 610M, Bruker Nano GmbH. EDS was used to conduct elemental analysis of the samples. The final concentration of each element was obtained by taking the average of measurements at different spots (at least 8).

X-ray fluorescence (XRF)

The chemical compositions of samples were measured by X-ray fluorescence (XRF, FISCHERSCOPE® X-RAY XDV®-SDD, Fischer Technology). In order to improve the precision of XRF analysis due to data scattering, 10 measurements for each sample were carried out. The Ca-Si-P wt% was estimated and then their's oxides calculated.

Microbiological study

Firstly, the 100 mg of every filler was mixed with 10 mL of MRS broth and incubated for 7 days at 30 ºC. Then the samples were collected to conduct microbiological analysis. For that *Lactobacillus paracasei* 3039 (from Polish Microorganisms Collection, Wroclaw, Poland) was used. The strain was cultivated in MRS broth (BTL Sp. z o.o., Łódź, Poland) for 24 h at 30 ºC, centrifuged and suspended in fresh MRS broth to obtain OD_{600} nm ca. 1.0. and added to MRS broth after filler incubation in ratio 1:3 (v/v).

Evaluation of microbial cells' viability was performed using 3-(4,5-dimethylthiazol-2-yl)-2,5-diphenyltetrazolium bromide assay (MTT). Total membrane permeability was tested by colorimetric measurements of the uptake of crystal violet solution by microbial cells. Cell surface hydrophobicity was analyzed by measuring the adsorption of Congo red dye on the surface of microbial cells. In all microbiological tests, the reference sample was the culture without any filler added [22].

Composites preparation

Three composites with different fillers were prepared. Each composite contained only one filler: HA, n-SiO2-HA, or SYL-HA. The volume fraction of a filler was constant, 55%. This volume fraction was established according to the handling properties of composite: it is the maximum filler content that does not worsen the mixing comfort of the uncured paste. To prepare the examined composites, the components of the organic matrix were mixed together, i.e. Bis-GMA and TEGDMA (3:2). 0.5% of each component of the initiating system (CQ and EDMAB) was added to the mixture. After thorough mixing, the appropriate amount of filler was added to maintain its 55% volume load. All components were further mixed to obtain a homogeneous paste. Then, the paste was placed into PTFE molds with the specific dimensions for each subsequent test (descriptions below), protected with the PET foil from both sides, and cured for 20 s from both sides (except samples for depth of cure) with the use of dental LED lamp

(DB-685, Coxo, the wavelength of the emitted light: 420-480 nm, emitted power > 1100 mW•cm^{-2}, diode power: max 5W).

Composites characterization

Degree of conversion (DC)

DC values were examined following the previously described method [23] using FT-IR Spectroscopy (Vertex70, Bruker Optics) in the ATR mode (diamond crystal). The tests were performed in the spectral range of 4000 – 600 cm^{-1} with a resolution of 4 cm^{-1} and 32 scans for signal accumulation. For each material, at least three samples of uncured paste and at least six samples (ϕ 4 mm, 4 mm thick) of cured composites were examined. DC was calculated from the following equation:

$$DC = \left(1 - \frac{R_{polymer}}{R_{monomer}}\right) \times 100 \qquad [\%]$$

where $R_{polymer}$ and $R_{monomer}$ are the ratios of the integral intensities of the band assigned to double methacrylic bonds (1638 cm^{-1}) reacting during the polymerization, to the integral intensities of the band assigned to C=C bonds in the aromatic ring that do not react during polymerization (1608 cm^{-1}), recorded in the polymer (after 20 s of curing) and monomer (before curing) spectra, respectively. Mean values and standard deviations were calculated.

Depth of cure (DOC)

DOC values were examined according to the ISO 4049:2019 [14] method. For this purpose, at least three samples of each material were prepared (ϕ 4 mm, multiple 4 mm thickness). The samples were cured of only one side. Immediately after curing, the part of the uncured material was scratched with the use of a spatula. Then, the thickness of the remaining material was measured with the digital caliper (±0.02 mm) in four places of the sample and divided by two. Mean values and standard deviations were calculated.

Opacity

The opacity was examined with the use of DT-145 colorimeter (Anticorr) for the samples prepared for SP and SL. Opacity was measured by taking the measure of the samples on a white and black background and background subtraction. Mean values and standard deviations were calculated.

Sorption (SP) and solubility (SL)

SP and SL values were examined after the 14-days incubation at 37 °C in deionized water (20 mL) and demineralizing solution (mL) according to the procedure described in ISO 4049:2019 [14]. The demineralizing solution was composed of 2.2 mM $CaCl_2$, 2.2 mM KH_2PO_4, and 0.05 M CH_3COOH. Its pH was regulated to 4.4 with the use of 1 M KOH. It is a typical solution that is commonly used to imitate cariogenic conditions [24]. This solution was applied to examine the impact of such aggressive

conditions on the SP and SL values, as well as other properties of the examined composites. Six samples of each material (ϕ 15 mm, 1 mm thick) were prepared and measured with the electronic caliper (±0.02 mm) in four places. Samples were stored at 37 °C in the presence of silica gel and weighed each day until the constant mass (±0.1 mg in 24 hours) was obtained (m_1). Then, three samples of each material were placed in deionized water, and three in the demineralizing solution for 14 days at 37 °C. After the incubation time, samples were surface dried with the blotting paper and weighed after 60 seconds (m_2). Then, samples were stored at 37 °C in the presence of silica gel and weighed each day until the constant mass (±0.1 mg in 24 hours) was obtained (m_3). SP and SL were calculated according to the following equations:

$$SP = \frac{m_2 - m_3}{v} \qquad [\mu g \cdot mm^{-2}]$$

$$SL = \frac{m_1 - m_3}{v} \qquad [\mu g \cdot mm^{-2}]$$

where V is the volume of a sample.

Mean values and standard deviations were calculated.

Flexural and compressive strength

Flexural and compressive strength were examined using the universal testing machine Zwick Z010 TN ProLine (Zwick Roell). Test parameters were selected on the basis of ISO 4049:2019 [14] for 3-point bend test (flexural strength) and [13] for compressive strength. At least ten samples of each material were prepared. Crosshead speed was set as 0.75 $mm \bullet min^{-1}$ for flexural strength and 1 $mm \bullet min^{-1}$ for compressive strength. In both cases, the initial force was 1 kgF. Samples for the flexural strength were rectangular (25 x 2 x 2 mm), while for the compressive strength they were cylindrical (ϕ 4 mm, 4 mm thick). The distance between the supports in the flexural strength tests was 20 mm. Mean values and standard deviations were calculated.

Calcium release

The concentrations of calcium released from the examined composites were examined in the solutions (deionized water and demineralized solution) after the incubation of samples for SP and SL. For this purpose, a combined ion-selective calcium electrode perfectION (Mettler Toledo) was applied. Three blank samples of deionized water and three blank samples of demineralizing solution stored in the same conditions as the examined solutions (the same vessels, 14 days at 37 °C) were also prepared and analyzed accordingly. For each 20 mL of the examined solution, 0.4 mL of ionic strength adjustment (TISAB) was added. According to the differences in the composites samples masses, the obtained concentration values were recalculated on the average sample mass, i.e. 350 mg.

Statistical analysis

The statistically significant differences in biological properties (cell viability, cell adhesion to Congo red, and cell membrane permeability) of the fillers were examined with the use of one-way variance analysis at a significance level of 0.05.

All results obtained for composites were subjected to statistical analysis. To examine the statistically significant differences in the values of DC, DOC, opacity, SP, SL, flexural strength, compressive strength, and Ca^{2+} concentrations one-way variance analysis was carried out at the significance level of 0.05. No statistically significant differences in the values of each parameter were denoted by the same capital letters in the figures or tables. Additionally, Student's t-tests (α=0.05) were conducted to examine the effect of the storing solution (water or demineralizing solution) in case of SP, SL, and Ca^{2+} release. No statistically significant differences in the values of each parameter were denoted by the same lower cases in the figures or tables. All calculations were performed with the use of Statistica 13.1 software (TIBCO Software).

Results And Discussion

Fillers

The first technique that confirms the effectiveness of creating hydroxyapatite-silica hybrid fillers is XRD (Fig. 3). The peaks seen for n-SiO2-HA and SYL-HA are in line with those of commercial hydroxyapatite (HA). Of course, they are not as sharp as in HA but this is due to the fact that the hydroxyapatite content is much lower in these fillers. In addition, broader peaks derived from hydroxyapatite may indirectly indicate the production of nanohydroxyapatite [25,26]. Another difference is the presence of a broad peak in the range 15-30 θ, which is characteristic of amorphous silica [27].

The efficiency of the filler synthesis is also visible in the FTIR spectra (Fig. 4). The most characteristic band proving the presence of hydroxyapatite is the band for vibrations from phosphate groups (PO_4^{3-}) [28,29]. This band is visible at 1021 cm^{-1} for HA, while at ~1030 cm^{-1} for n-SiO2-HA and SYL-HA. For silica-hydroxyapatite fillers, the band is much wider and this is due to the overlap of the phosphate band with the stretching vibration band of Si-O-Si. Despite the overlap of the two bands, the sharp band for PO_4^{3-} is clearly visible.

The morphology of all fillers was assessed on the basis of SEM images (Fig 5.). The hydroxyapatite (HA) filler particles are non-uniform in shape and size. There are visible cuboidal and plate-shaped particles. In the case of the n-SiO2-HA filler, single particles cannot be distinguished, only large clusters of nanoparticles are visible. Particles of uniform size can be observed for the SYL-HA filler. The most important information obtained from the SEM images is that both in n-SiO2-HA and SYL-HA there are no distinct areas that would indicate the formation of separate silica and hydroxyapatite.

Even more detailed information on the distribution of hydroxyapatite and silica was obtained by EDS analysis (Fig. 6). As can be seen in the case of both synthesized fillers, both components (hydroxyapatite and silica) are evenly distributed as evidenced by the distribution of Ca, P, and Si. It is not surprising that commercial hydroxyapatite (HA) has the highest calcium (36%) and phosphorus (16%) content. Interestingly, both synthesized fillers, despite different methods of their preparation, have similar contents of calcium, phosphorus and silicon. It is very important that there are no places where a very large amount of silicon or calcium and phosphorus is visible. The lack of such places indirectly proves the high homogeneity of the obtained fillers. Obtaining fillers with an even distribution of both elements is important because the composite prepared from them should have the same mechanical properties and remineralization potential in each place.

XRF results also indicate a similar calcium content in the n-SiO2-HA and SYL-HA samples (Table 1). Due to this, the same amounts of remineralizing agent (Ca^{2+}) can be released from both new fillers. In commercial hydroxyapatite, the content of calcium and phosphorus is higher than in the obtained fillers.

Table 1. XRF analysis results showing the composition of tested fillers.

	HA	n-SiO2-HA	SYL-HA
CaO	63.11%	22.76%	24.71%
P_2O_5	35.36%	15.71%	21.26%
SiO_2	0.59%	59.17%	50.98%

Cells of the probiotic strain *Lactobacillus paracasei* 3039 were analyzed for changes in metabolic activity (cell viability), adhesion properties, and cell membrane permeability. The collected results clearly indicate that the tested fillers, i.e. hydroxyapatite and silica-hydroxyapatite materials, did not show toxic effects on microorganisms and no negative effects on the other tested parameters were observed. Thus, a negative effect on probiotic bacteria can be excluded.

Interactions between *Lactobacilli* and hydroxyapatite and derivatives based on it have been studied, although the question of toxicity has not been analyzed and authors have usually focused on cell adhesion to the material [30,31]. However, the information on ion release from hydroxyapatite required studying this issue to be sure that all tested fillers are safe against probiotic bacteria that are present in the gastrointestinal tract and may be exposed to ions released e.g. in the oral cavity [32].

Table 2. Mean values (±SD) of cell viability, cell adhesion to Congo red, and cell membrane permeability (the same capital letters in rows (A, B) mean no statistically significant differences ($p > 0.05$) in values of examined parameters).

	control	HA	n-SiO2-HA	SYL-HA
cell viability [%]	100 (±9)^{A}	104 (±1)^{A}	92 (±6)^{A}	155 (±3)^{B}
cell adhesion to Congo red [%]	12 (±0)^{A}	10 (±3)^{A}	8 (±5)^{A}	5 (±3)^{A}
cell membrane permeability [%]	11 (±1)^{A}	12 (±5)^{A}	11 (±2)^{A}	29 (±0)^{B}

Composites

As the filler type is the only variable in the composition of the tested composites, in order to simplify the reading of the results, the names of the composites come from the type of the applied filler.

Typically, DC values of Bis-GMA-based composites are in the range of 52 to 75%, while the 55 % value is considered the lower limit for the occlusal restorations [33]. All examined composites show mean DC values far above 55% (Fig. 7).

Mean values (±SD) of this parameter are 76.0 (±8.2), 82.7 (±14.4), and 74.9 (±6.2)% for HA, n-SiO2-HA, and SYL-HA, respectively. There are no statistically significant differences in the DC values between the examined composites, so it can be stated that in this case, the effect of the filler type is negligible.

The second parameter related to the curing of the composites that was examined is DOC. Its values are presented in Fig. 8. DOC examination consists of scratching of the uncured part of the composite, that was cured of only one side. This one-sided light exposure causes that DOC values differentiate better the effect of the applied filler on the curing.

Mean DOC values (±SD) are 3.41 (±0.09), 5.07 (±0.18), and 2.77 (±0.32) mm for HA, n-SiO2-HA, and SYL-HA, respectively. First of all, all these composites meet ISO 4049:2019 criteria for opaque (1 mm) and other restorative materials (1.5 mm) in terms of DOC [14]. The differences observed between the materials are statistically significant ($p < 0.05$). The highest DOC is observed in n-SiO2-HA, while the smallest depth shows SYL-HA. These differences probably result from different optical properties of the applied fillers, especially the refractive index, as well as particle size. Higher resin and filler refractive index differences result in lower light transmittance through the hardened paste, which causes lower DOC values, as well as higher opacity of the composite [34]. A clear correlation between DOC and opacity is observed (Table 3). The lowest opacity shows n-SiO2-HA composite, while the highest opacity is observed for SYL-HA. The differences in the opacity values are statistically significant ($p < 0.05$). Lower opacity corresponds with the higher DOC.

Table 3. Mean values (±SD) of opacity, sorption (SP), and solubility (SL) of examined composites (the same capital letters in rows (A, B, C) mean no statistically significant differences ($p > 0.05$) in values of examined parameters; the same lower case in columns (a, b, c, d, e, f) mean no statistically significant differences ($p > 0.05$) in values of SP and SL in deionized water and demineralizing solution)

	COMPOSITE		
	HA	n-SiO2-HA	SYL-HA
Opacity [%]	59.9 (±2.9)^{A}	48.9 (±4.8)^{B}	65.9 (±1.8)^{C}
SP (deionized water) [μg•mm^{-2}]	52.18 (±2.75)^{A,a}	45.21 (±0.65)^{A,b}	50.92 (±4.59)^{A,c}
SP (demineralizing solution) [μg•mm^{-2}]	47.73 (±2.87)^{A,a}	45.85 (±2.22)^{A,b}	50.33 (±1.21)^{A,c}
SL (deionized water) [μg•mm^{-2}]	-1.22 (±0.32)^{B,d}	-5.66 (±0.52)^{A,e}	-6.81 (±0.90)^{A,f}
SL (demineralizing solution) [μg•mm^{-2}]	0.19 (±2.44)^{B,d}	-6.40 (±0.65)^{A,e}	-7.38 (±1.44)^{A,f}

The amount of the light that is transmitted through the irradiated material and DOC values depend also on the fillers particle size. DOC became shallower when the filler particle size increases [35]. The obtained results are consistent with this finding, as the n-SiO2-HA filler is nano-sized, while HA and SYL-HA fillers are micro-sized.

The maximum values of SP and SL defined by ISO 4049:2019 are ≤ 40 and ≤ 7.5 μg•mm^{-2}, respectively [14]. All examined composites show higher values of SP (Table 3), thus not meeting the conditions of the ISO. There are no statistically significant differences in the SP values depending on the filler type, as well as solution i.e. deionized water or demineralizing agent. No effect of the solvent type is optimistic, as it was predicted that the cariogenic demineralizing solution act more aggressively than the water.

SL values of all examined composites are lower than 7.5 μg•mm^{-2}, but they are mostly negative (Table 3). It means that their m_3 was higher than m_1, so the materials strongly absorbed the fluids from their surroundings during the incubation. This absorption prevails over the solubility. No effect of the solvent type was observed, which, one more time, is a positive observation. The effect of the filler type can be observed. HA-filled composite shows lower SL absolute values in both solvents. Probably the presence of the silica in n-SiO2-HA and SYL-HA results in the stronger irreversible bonding of the water by the composites. It is not surprising, as silica is strongly hydrophilic. To overcome this weak mass stability of the examined composites in the future, fillers silanization or hydrophobization is recommended.

Minimum flexural strength values for class 2, group 1 polymer-based restorative materials that are intended to restore the occlusal and other surfaces of teeth are defined by ISO 4049:2019 as 80 and 50 MPa, respectively [14]. Class 2, group 1 restorations are defined as materials cured intra-orally that require the external source of energy, e.g. blue light-emitting lamp [14], therefore, the examined materials fit into this criterion. Flexural strength values of the examined composites are presented in Fig. 9.

Mean values (±SD) of flexural strength of examined composites are 71.56 (±6.27), 53.08 (±1.54), and 60.37 (±1.54) for HA, n-SiO2-HA, and SYL-HA, respectively. HA-filled composite show statistically significantly higher value of this parameter than silica-HA-filled composites (n-SiO2-HA and SYL-HA). There are no difference in flexural strength between n-SiO2-HA and SYL-HA ($p > 0.05$).

It may be related to the smaller particle size of silica-HA fillers (nano for n-SiO2-HA and 2-3 μm for Syloid 244) compared to HA (c.a. 10 μm). Smaller filler particles create a larger contact surface with the components of the organic matrix. It causes the "saturation" of the resin and forming the cracks on the filler/matrix interface during tests where the bending load is applied [36]. Unfortunately, none of the examined materials is appropriate for the restoration of occlusal surfaces of teeth, as their flexural strength values are lower than 80 MPa. However, they all meet the criterion for the restoration of non-occlusal surfaces exceeding the value of 50 MPa.

The compressive strength of dentin and enamel is 297 and 384 MPa, respectively [6]. Mean values (±SD) of this parameter of examined composites are 292.58 (±18.82), 402.27 (±29.93), and 269.27 (±27.96) for HA, n-SiO2-HA, and SYL-HA, respectively (Fig. 10). There are no statistically significant differences in compressive strength between HA and SYL-HA, while the value of this parameter obtained for n-SiO2-HA is significantly higher.

Considering the mean values of compressive strength, together with the standard deviations it can be cautiously assumed that HA and SYL-HA compressive strengths are very close to the compressive strength of dentin. However, the values of this parameter for both mentioned materials are far lower than the compressive strength of enamel. Therefore, in terms of this parameter, both materials could be considered as appropriate to restore dentin, but inappropriate to restore enamel. The compressive strength of n-SiO2-HA, which is higher than the compressive strength of both discussed tissues, can ensure success in restoring enamel and dentin. The higher value of compressive strength of n-SiO2-HA in comparison with HA and SYL-HA results probably from the smaller particle size of n-SiO2-HA. In general, it is a rule that nanocomposites show higher compressive strength than composites with greater particles [6]. The values of compressive strength show positive correlation with the values of DOC and opacity, i.e. materials showing lower opacity show higher compressive strength and DOC.

Mean values (±SD) of calcium concentration detected in the deionized water after incubation the samples of the examined materials are 1.94 (±0.27), 0.63 (±0.33), and 1.13 (±0.13) ppm for HA, n-SiO2-HA, and SYL-HA, respectively (Fig. 11). HA shows a significantly ($p < 0.05$) higher amount of calcium released during incubation in deionized water, while the differences between both silica-HA-filled composites (n-SiO2-HA and SYL-HA) are statistically insignificant ($p > 0.05$). It is not surprising that HA-filled composite is the most effective in the Ca^{2+} releasing as the only filler in this composite is HA. In contrast, both remaining composites contain also silica, so the amount of calcium-bearing filler is obviously smaller. In all cases, incubation of the samples in the demineralizing solution that imitates the cariogenic environment results in higher calcium concentrations. These differences are statistically significant for all examined materials (different lower cases). Mean values (±SD) of calcium concentration detected in the demineralizing solution after incubation the samples of the examined materials are 7.13 (±1.64), 7.06 (±0.35), and 6.62 (±0.62) ppm for HA, n-SiO2-HA, and SYL-HA, respectively (Fig. 11). There are no statistically significant differences ($p > 0.05$) in the values of Ca^{2+} concentrations between all examined materials. Higher concentrations of calcium in demineralizing solution in comparison with deionized water results probably from the presence of phosphate ions in the

demineralizing solution. The research proves that PO_4^{3-} ions in the solution increase the solubility of Ca^{2+} ions included in the hydroxyapatite. This phenomenon is explained by the formation of complexes of calcium phosphates such as $Ca(HPO_4)(H_2PO_4)^-$ and $Ca(H_2PO_4)OH$ [37]. This increase of the Ca^{2+} solubility is relatively small compared to the total weight of the composite, therefore, it is not reflected in the SL values. Since HA is bounded to silica only by physical interactions in silica-hydroxyapatite materials, the formation of complexes with phosphates contained in the demineralization solution probably exceeds the strength of these interactions, resulting in the equalization of Ca^{2+} ion release capacity by all tested composites.

The increased ability of tested materials to release Ca^{2+} in demineralizing solution in comparison with deionized water should be considered beneficial. It means that the cariogenic environment activates the anticaries mechanisms, understood as the ability to Ca^{2+} release with no significant mass loss of the composite.

Conclusions

Both silica-hydroxyapatite hybrid fillers were prepared successfully. Their homogeneity and non-toxicity were proved allowing, therefore, the application in the potential dental restorations. Among these two prepared hybrid fillers, nano-sized silica that was co-synthesized with HA (n-SiO2-HA) proved to be better than SYLOID®244 with HA layer (SYL-HA). RBC filled with n-SiO2-HA showed better DOC and compressive strength in comparison with HA-filled RBC, simultaneously maintaining the remineralization potential understood as the ability to release calcium ions. Therefore, the research hypothesis is partially confirmed. However, it has to be also partially rejected as the flexural strength of n-SiO2-HA composite was lower than that of the HA composite. This property has to be further improved as it is still too low to meet the ISO 4049:2019 criterion for the occlusal restorations. In the context of using the second hybrid filler (SYL-HA), the research hypothesis must be rejected in its entirety, as SYL-HA-filled RBC showed inferior mechanical properties in comparison with HA-filled RBC. Despite that the mass stability (SP and SL) during incubation of all examined composites was the same, it has to be also improved as it is lower than acceptable. Probably, mixing the fillers with different particle sizes or silanization may improve the flexural strength of the composites. As all materials were rather hydrophilic, the filler's surface hydrophobization may in turn result in the mass stability improvement. Therefore, despite the obtained results are very perspective, further experiments are required.

Declarations

Funding

This work was supported by the Ministry of Education and Science.

Competing Interests

The authors have no relevant financial or non-financial interests to disclose.

Data Availability

The datasets generated during and/or analysed during the current study are available from the corresponding author on reasonable request.

Acknowledgement

This work was supported by the Ministry of Education and Science.

References

1. S.V. Dorozhkin, M. Epple, Biological and Medical Significance of Calcium Phosphates. Angew. Chem. Int. Edit. **41**, 3130–3146 (2002)
2. S.V. Dorozhkin, Bioceramics of calcium orthophosphates. Biomaterials **31**, 1465–1485 (2010)
3. S.V. Dorozhkin, Calcium orthophosphates in dentistry. J. Mater. Sci. – Mater. M. **24**, 1335–1363 (2013)
4. C. Xie, H. Lu, W. Li, F.M. Chen, Y.M. Zhao, The use of calcium phosphate-based biomaterials in implant dentistry. J. Mater. Sci. – Mater. M. **23**, 853–862 (2012)
5. R.R. Braga, Calcium phosphates as ion-releasing fillers in restorative resin-based materials. Dent. Mater. **35**, 3–14 (2019)
6. R.L. Sakaguchi, J.M. Powers (eds.), *Craig's Restorative Dental Materials, Thirteenth Edition* (Elsevier, 2012)
7. P. Laurance-Young, L. Bozec, L. Gracia, G. Rees, F. Lippert, R.J.M. Lynch, J.C. Knowles, A review of the structure of human and bovine dental hard tissues and their physicochemical behaviour in relation to erosive challenge and remineralisation. J. Dent. **39**, 266–272 (2011)
8. M.A. Meyers, P.Y. Chen, A.Y.M. Lin, Y. Seki, Biological materials: Structure and mechanical properties. Prog. Mater Sci. **53**, 1–206 (2008)
9. I.M. Low, N. Duraman, U. Mahmood, Mapping the structure, composition and mechanical properties of human teeth. Mat. Sci. Eng. C **28**, 243–247 (2008)
10. Z. Okulus, T. Buchwald, A. Voelkel, Calcium release from experimental dental materials. Mat. Sci. Eng. C **68**, 213–220 (2016)
11. Z. Okulus, T. Buchwald, A. Voelkel, Characterization of light-cured, dental-resin-based biocomposites. J. Appl. Polym. Sci. **132**, 42812 (1–10) (2015)
12. E. Ali Abou Neel, A. Aljabo, A. Strange, S. Ibrahim, M. Coathup, A.M. Young, L. Bozec, V. Mudera, Demineralization–remineralization dynamics in teeth and bone. Int. J. Nanomed. **11**, 4743–4763 (2016)

13. Z. Okulus, A. Voelkel, Mechanical properties of experimental composites with different calcium phosphates fillers. Mat. Sci. Eng. C **78**, 1101–1108 (2017)
14. ISO 4049:2019: Dentistry-Polymer-based restorative materials
15. B. Pratap, R.K. Gupta, B. Bhardwaj, M. Nag, Resin based restorative dental materials: characteristics and future perspectives. Jpn. Dent. Sci. Rev. **55**, 126–138 (2019)
16. E.G. Habib, R. Wang, Y. Wang, M. Zhu, X.X. Zhu, Inorganic Fillers for Dental Resin Composites - Present and Future. ACS Biomater. Sci. Eng. **2**, 1–11 (2016)
17. M. Sandomierski, Z. Buchwald, T. Buchwald, A. Voelkel, Silica-filled methacrylic composites with extremely high compressive strength. J. Mech. Behav. Biomed. **116**, 104319 (2021)
18. Z. Okulus, M. Sandomierski, M. Zielińska, T. Buchwald, A. Voelkel, Zeolite fillers for resin-based composites with remineralizing potential. Spectrochim. Acta A **210**, 126–135 (2019)
19. Z. Buchwald, M. Sandomierski, A. Voelkel, Calcium-Rich 13X Zeolite as a Filler with Remineralizing Potential for Dental Composites, ACS Biomater. Sci. Eng. **6**, 3843–3854 (2020)
20. M. Sandomierski, Z. Buchwald, A. Voelkel, Calcium montmorillonite and montmorillonite with hydroxyapatite layer as fillers in dental composites with remineralizing potential. Appl. Clay Sci. **198**, 105822 (2020)
21. X. Hao, X. Hu, C. Zhang, S. Chen, Z. Li, X. Yang, H. Liu, G. Jia, D. Liu, K. Ge, X.-J. Liang, J. Zhang, Hybrid Mesoporous Silica-Based Drug Carrier Nanostructures with Improved Degradability by Hydroxyapatite. ACS Nano **9**, 9614–9625 (2015)
22. A. Pacholak, W. Smułek, A. Zgoła-Grześkowiak, E. Kaczorek, Nitrofurantoin—Microbial Degradation and Interactions with Environmental Bacterial Strains. Int. J. Env. Res. Pub. He. **16**, 1526 (2019)
23. Z. Okulus, T. Buchwald, M. Szybowicz, A. Voelkel, Study of a new resin-based composites containing hydroxyapatite filler using Raman and infrared spectroscopy. Mater. Chem. Phys. **145**, 304–312 (2014)
24. T. Buchwald, Z. Buchwald, Assessment of the Raman spectroscopy effectiveness in determining the early changes in human enamel caused by artificial caries. Analyst **144**, 1409–1419 (2019)
25. J. Zhang, Y. Zhao, B. Palosz, Comparative studies of compressibility between nanocrystalline and bulk nickel. Appl. Phys. Lett. **90**, 1–3 (2007)
26. S.M. Londoño-Restrepo, R. Jeronimo-Cruz, B.M. Millán-Malo, E.M. Rivera-Muñoz, M.E. Rodriguez-García, Effect of the Nano Crystal Size on the X-ray Diffraction Patterns of Biogenic Hydroxyapatite from Human, Bovine, and Porcine Bones. Sci. Rep. **9**, 5915 (2019)
27. R. Maddalena, C. Hall, A. Hamilton, Effect of silica particle size on the formation of calcium silicate hydrate[C-S-H] using thermal analysis. Thermochim. Acta **672**, 142–149 (2019)
28. A. Zima, Hydroxyapatite-chitosan based bioactive hybrid biomaterials with improved mechanical strength. Spectrochim. Acta A **193**, 175–184 (2018)
29. C.C. Coelho, L. Grenho, P.S. Gomes, P.A. Quadros, M.H. Fernandes, Nano-hydroxyapatite in oral care cosmetics: characterization and cytotoxicity assessment. Sci. Rep. **9**, 11050 (2019)

30. H. Jalasvuori, A. Haukioja, J. Tenovuo, Probiotic Lactobacillus reuteri strains ATCC PTA 5289 and ATCC 55730 differ in their cariogenic properties in vitro. Arch. Oral Biol. **57**(12), 1633–1638 (2012)
31. S.C. Venegas, J.M. Palacios, M.C. Apella, P.J. Morando, M.A. Blesa, Calcium Modulates Interactions between Bacteria and Hydroxyapatite. J. Dent. Res. **85**(12), 1124–1128 (2006)
32. A. Mocanu, O. Cadar, P.T. Frangopol, I. Petean, G. Tomoaia, G.A. Paltinean, C.P. Racz, O. Horovitz, M. Tomoaia-Cotisel, Ion release from hydroxyapatite and substituted hydroxyapatites in different immersion liquids: in vitro experiments and theoretical modelling study R. Soc. Open Sci. **8**(1), 201785 (2021)
33. R.Z. Alshali, N. Silikas, J.D. Satterthwaite, Degree of conversion of bulk-fill compared to conventional resin-composites at two time intervals. Dent. Mater. **29**, 213–217 (2013)
34. A.C. Shortall, W.M. Palin, P. Burtscher, Refractive Index Mismatch and Monomer Reactivity Influence Composite Curing Depth. J. Dent. Res. **87**, 84–88 (2008)
35. K. Fujita, T. Ikemi, N. Nishiyama, Effects of particle size of silica filler on polymerization conversion in a light-curing resin composite. Dent. Mater. **27**, 1079–1085 (2011)
36. I. Ikejima, R. Nomoto, J.F. McCabe, Shear punch strength and flexural strength of model composites with varying filler volume fraction, particle size and silanization. Dent. Mater. **19**, 206–211 (2003)
37. Z.F. Chen, B.W. Darvell, V.W.H. Leung, Hydroxyapatite solubility in simple inorganic solutions. Arch. Oral Biol. **49**, 359–367 (2004)

Figures

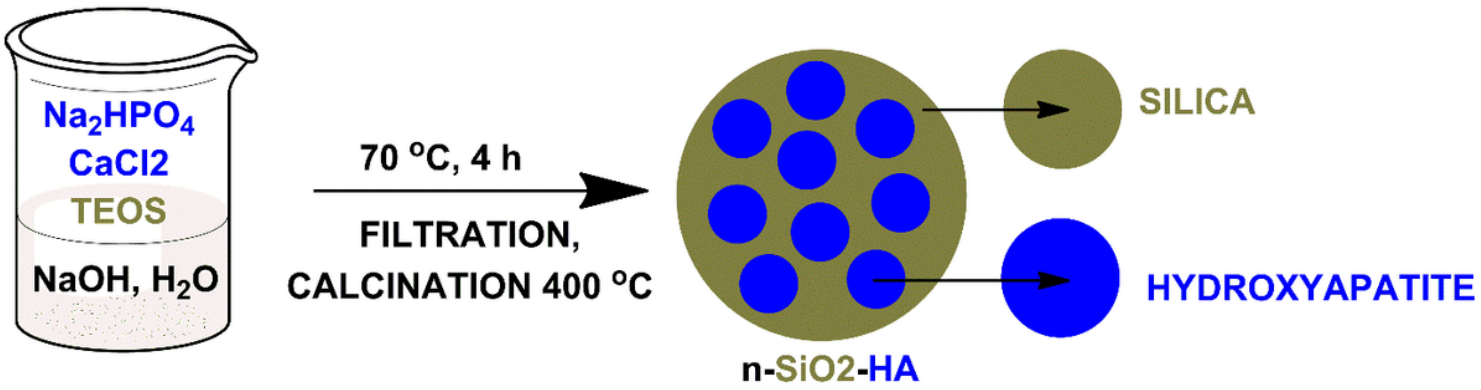

Figure 1

The scheme of n-SiO2-HA synthesis.

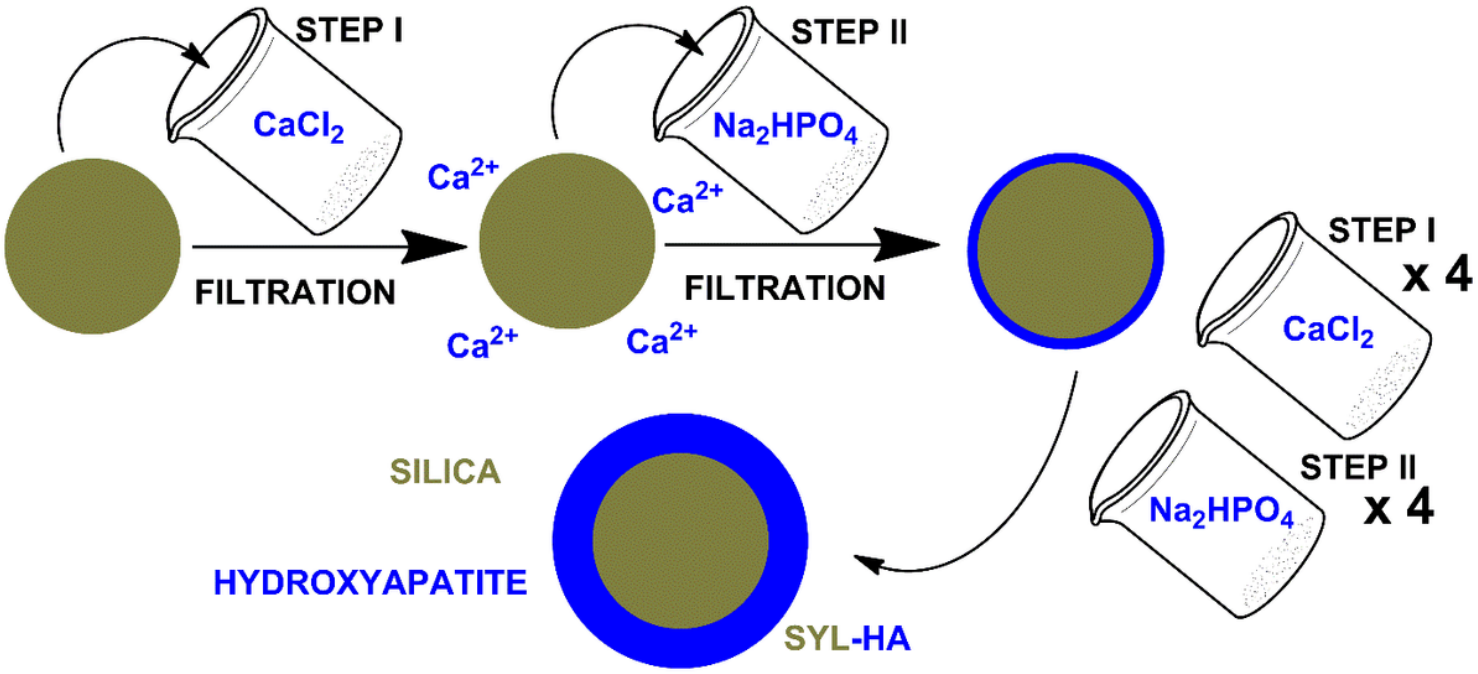

Figure 2

The scheme of SYL-HA preparation.

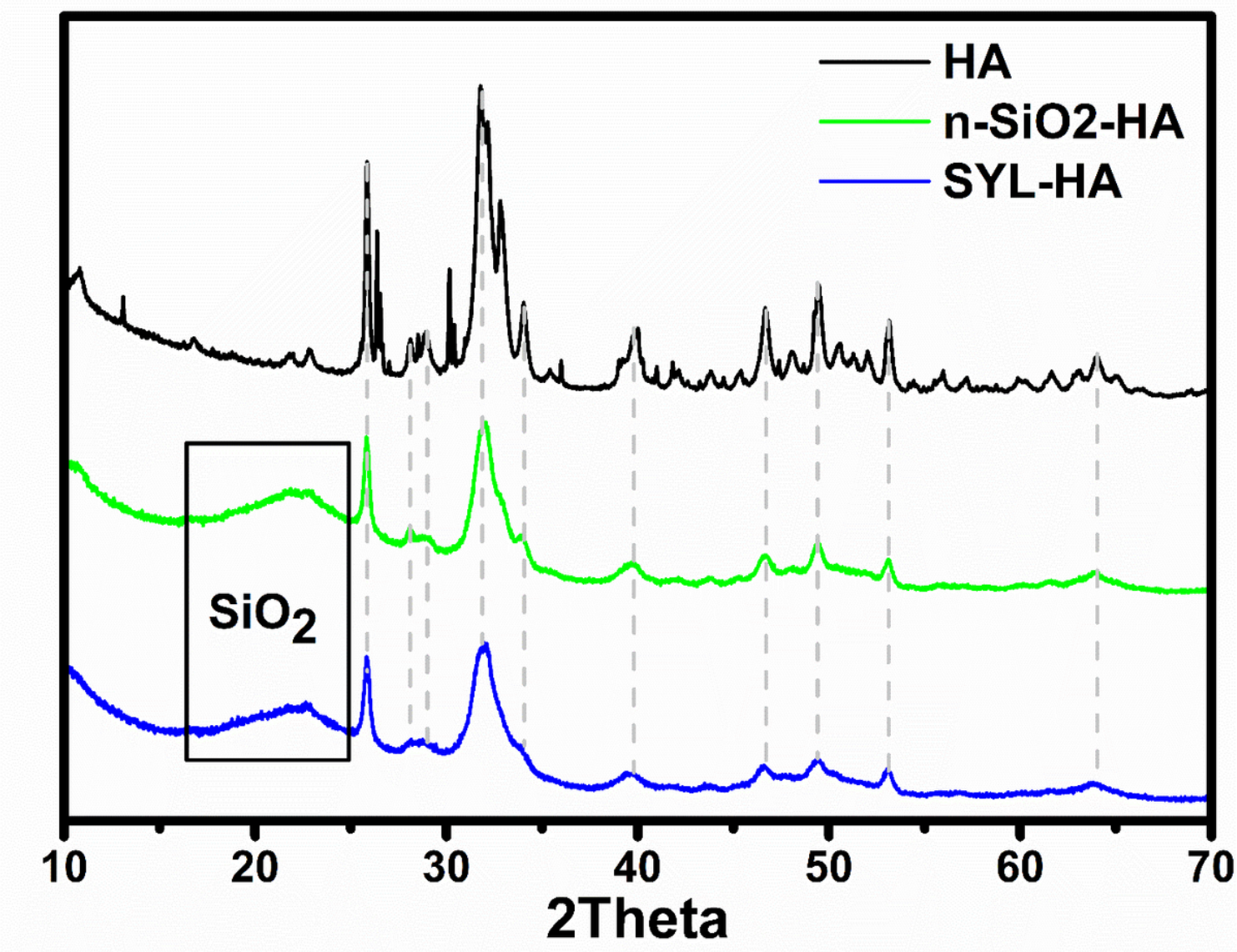

Figure 3

X-ray diffraction patterns of HA, n-SiO2-HA, and SYL-HA.

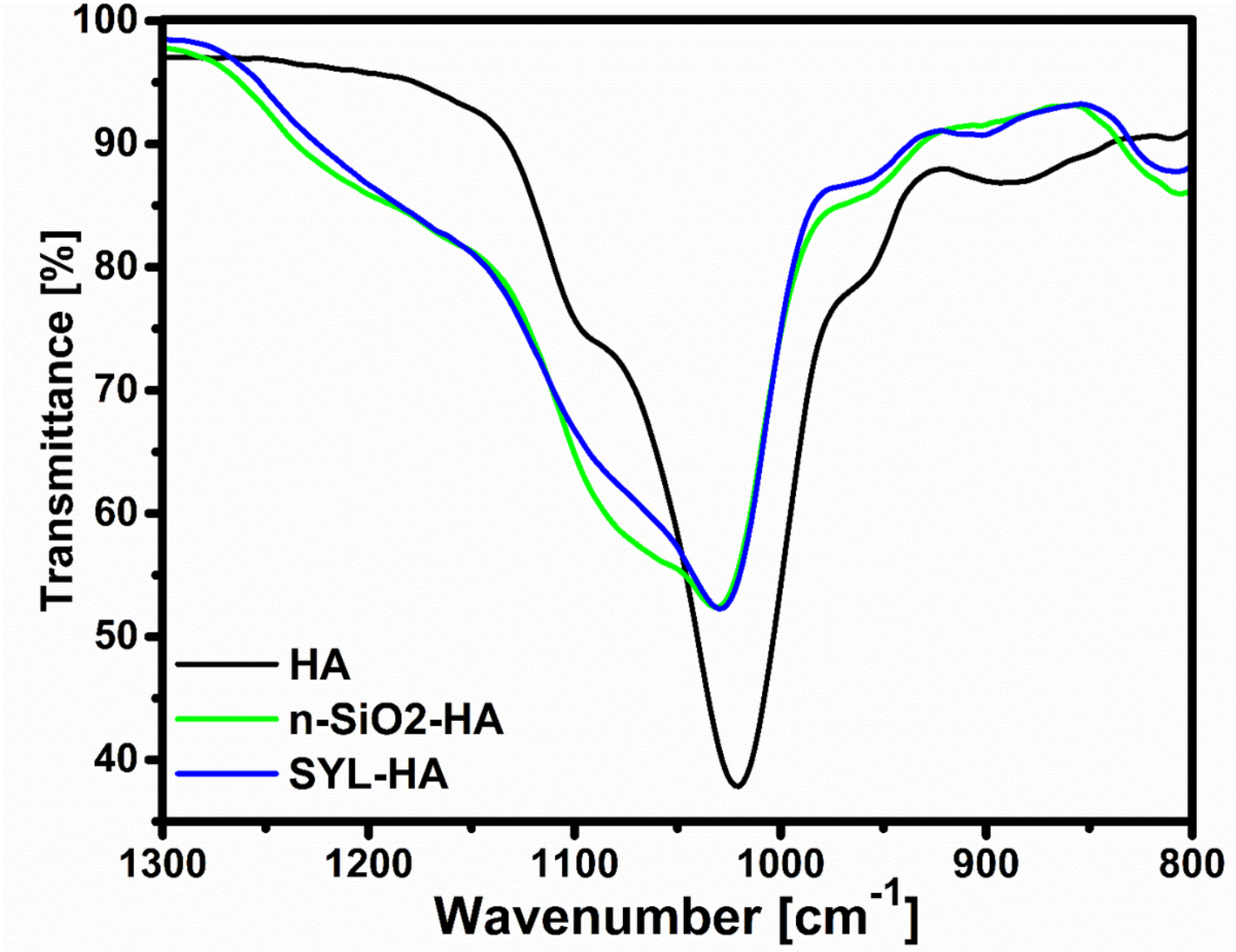

Figure 4

FT-IR spectra of HA, n-SiO2-HA, and SYL-HA fillers.

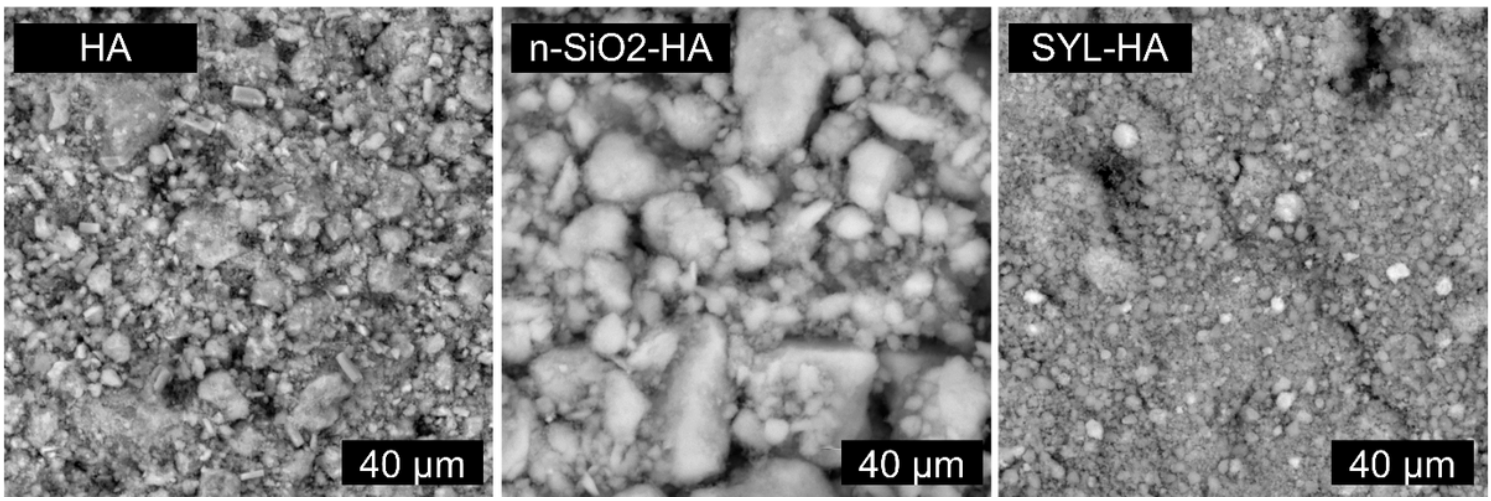

Figure 5

SEM images of HA, n-SiO2-HA, and SYL-HA fillers.

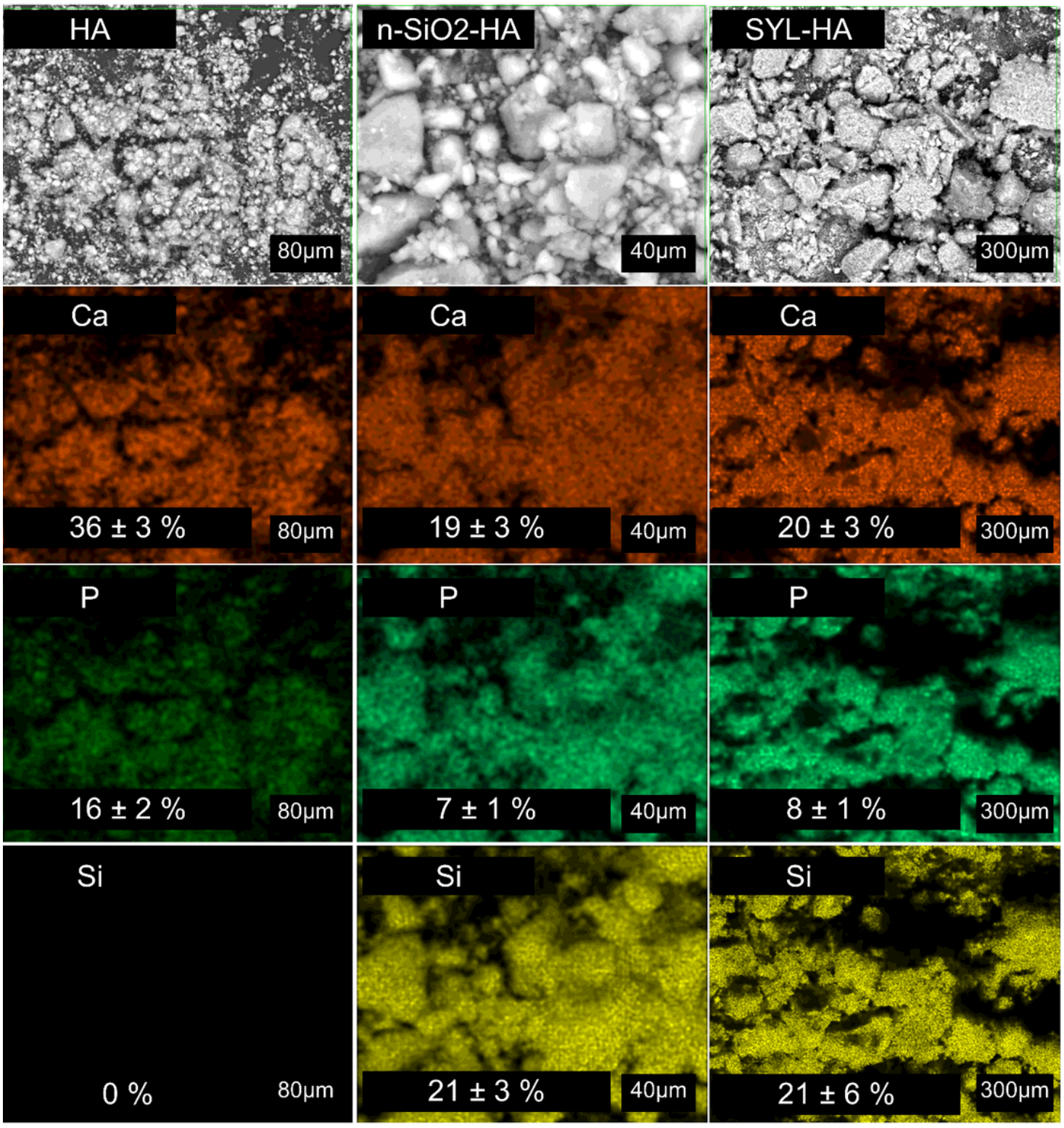

Figure 6

SEM images of fillers (first row). Elemental mapping of the same regions indicating spatial distribution of calcium (second row), phosphorus (third row), and silicon (fourth row). The values represent the content of elements in the filler (by weight).

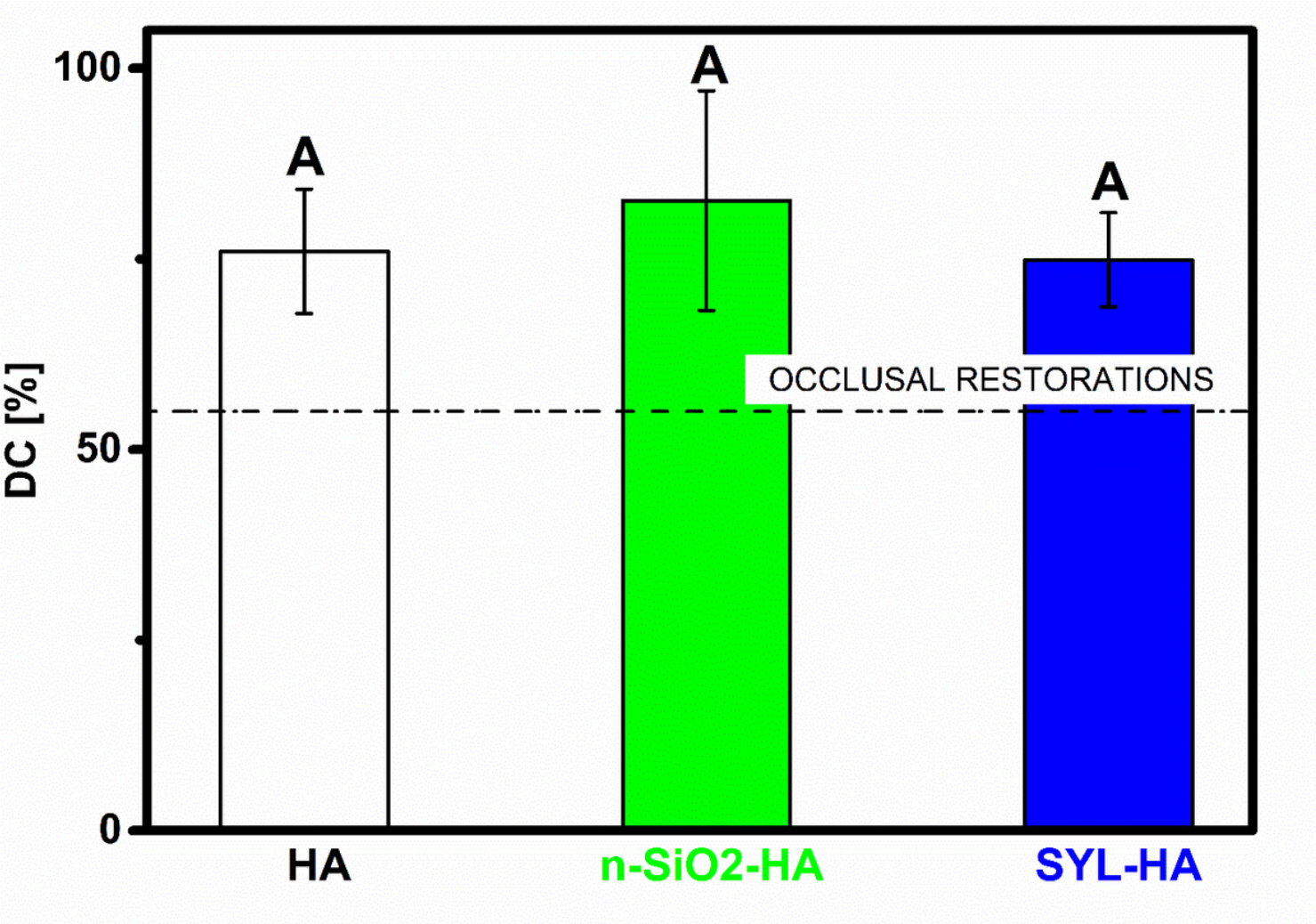

Figure 7

Mean values of DC of examined composites (error bars present the values of standard deviation; dotted line presents the critical value for occlusal restorations (55%) [33]; the same capital letters (A) mean no statistically significant differences ($p > 0.05$) in values of DC).

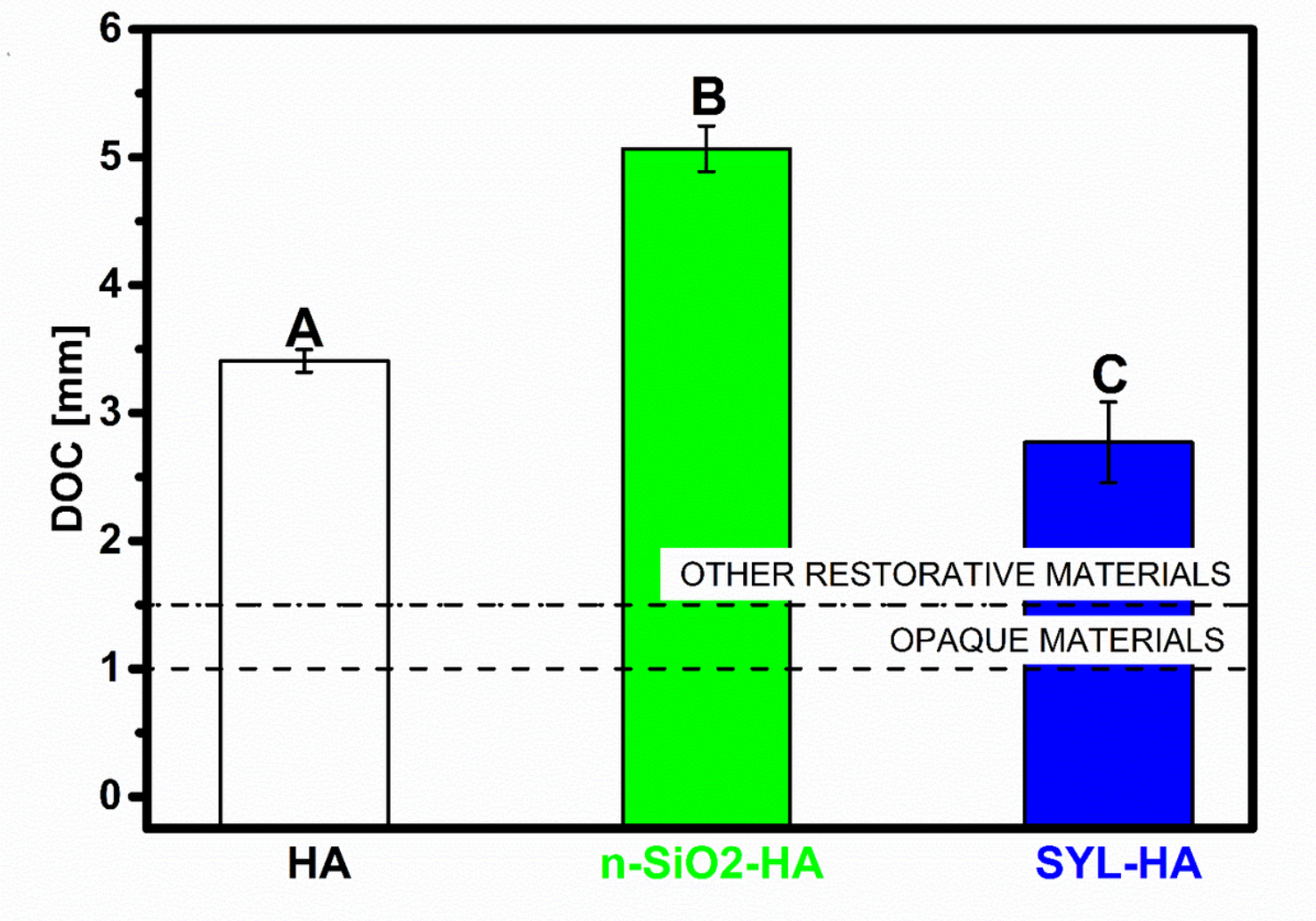

Figure 8

Mean values of DC of examined composites (error bars present the values of standard deviation; dotted lines present the ISO 4049:2019 requirements [14]; the same capital letters (A, B, C) mean no statistically significant differences ($p > 0.05$) in values of DOC).

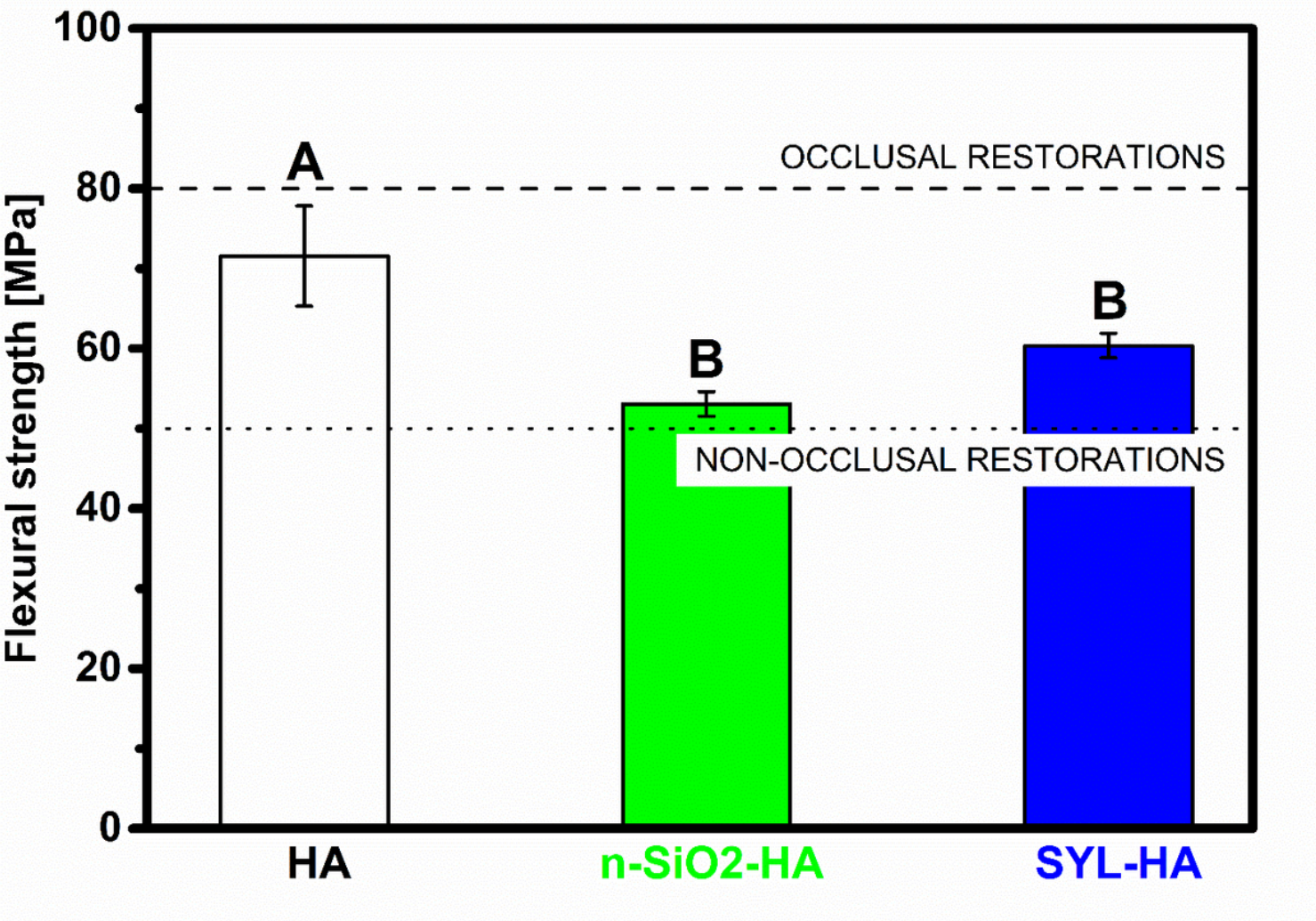

Figure 9

Mean values of flexural strength of all examined composites (error bars present the values of standard deviation; dotted lines present the ISO 4049:2019 requirements [14]; the same capital letters (A, B) mean no statistically significant differences ($p > 0.05$) in values of flexural strength).

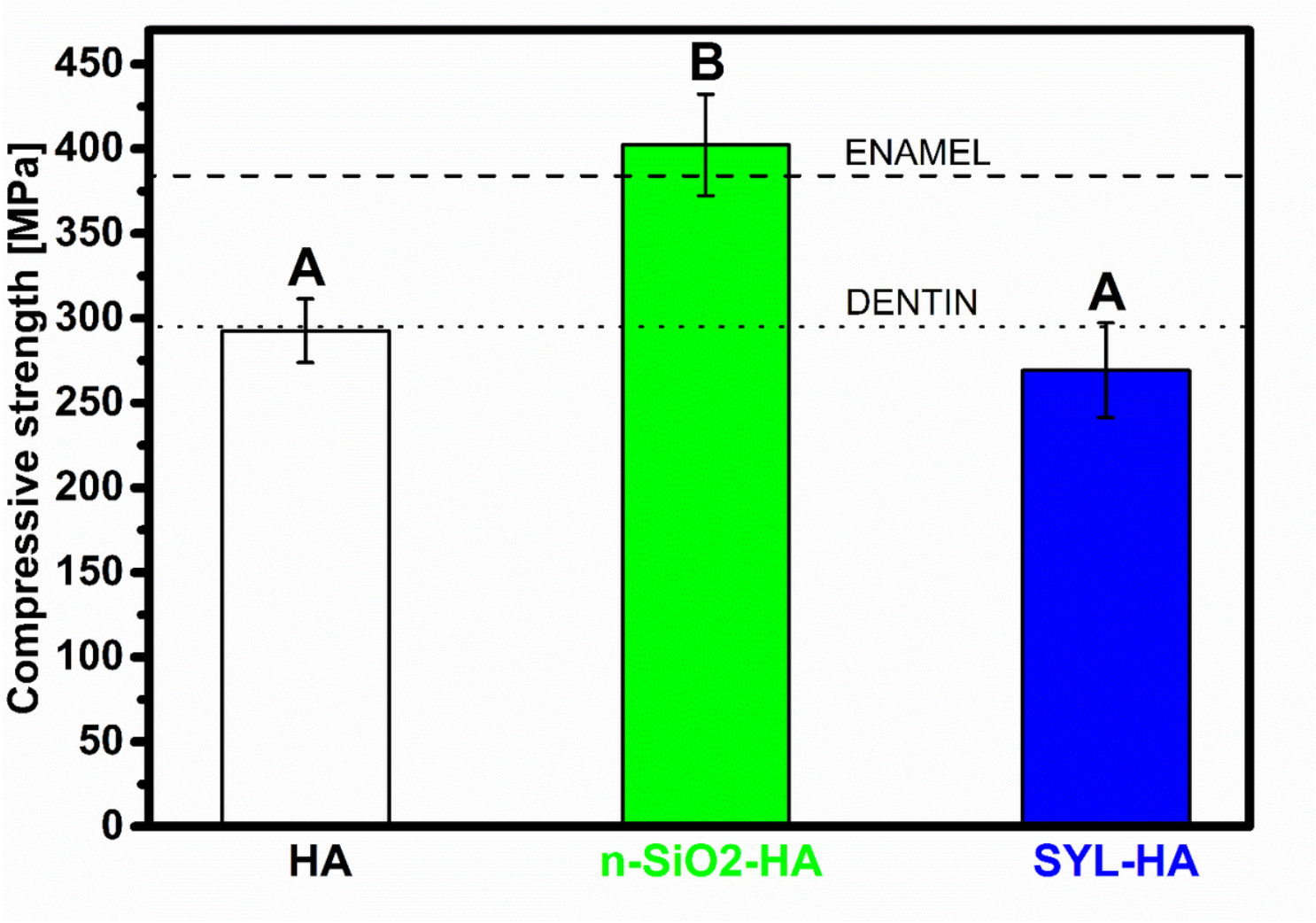

Figure 10

Mean values of compressive strength of all examined composites (error bars present the values of standard deviation; dotted lines present the compressive strength of dentin and enamel; the same capital letters (A, B) mean no statistically significant differences ($p > 0.05$) in values of compressive strength).

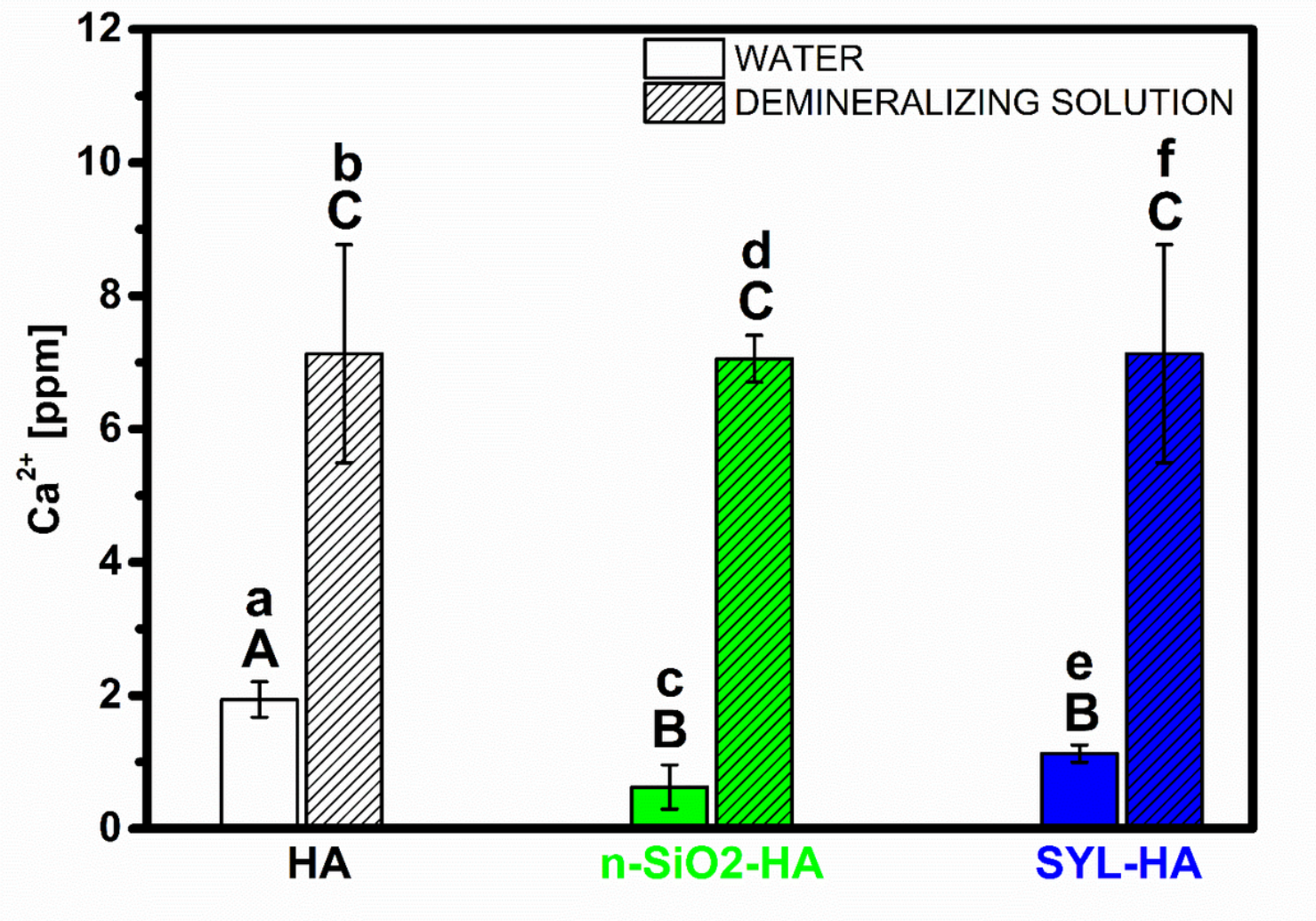

Figure 11

The concentration of calcium ions released by the examined composites recalculated on the average sample mass, i.e. 350 mg (mean values, error bars present the values of standard deviation; the same capital letters (A, B, C) mean no statistically significant differences ($p > 0.05$) in values of Ca^{2+} concentrations – calculated separately for deionized water and demineralizing solution; the same lower cases (a, b, c, d, e, f) mean no statistically significant differences ($p > 0.05$) in values of Ca^{2+} concentrations – calculated in pairs in which the type of the solution was set as variable, while the material type was constant).

Supplementary Files

This is a list of supplementary files associated with this preprint. Click to download.

- Onlinefloatimage12.png